Tutors

Dr. Carlos María Müller Jevenois
Departament de Ciència de Materials i Química Física

Dra. Gabriela Calderó Linnhoff
IQAC - CSIC

Grau de Química

Treball Final de Grau

Preparació i caracterització de nanopartícules polimèriques catiòniques i estudi de la seva interacció amb seroalbúmina.

Synthesis and characterization of cationic polymer nanoparticles and investigation of their interaction with seroalbumin.

Adrián Fernández Córdoba

June 2018

Universitat de Barcelona

B:KC Barcelona Knowledge Campus
Campus d'Excel·lència Internacional

Li estic infinitament agraït al Mateu, per tot els ànims que m'ha donat durant aquests mesos i des de sempre. Tot i les circumstàncies per les quals estic passant ara mateix, m'has donat forces per acabar aquest treball. Gràcies.

També voldria donar les gràcies a la Gaby, per tots els seus consells i pel seu optimisme durant la realització d'aquest treball.

REPORT

CONTENTS

1. SUMMARY

Today, a big pharmaceutical research effort is dedicated to controlled and targeted release of drugs. One of the most innovative options is the use of nanoparticles as non-viral vectors for the controlled and/or targeted release of drugs towards target organs or tissues. In these fields, the use of polymer nanoparticles is widespread due to their versatility: they can be easily functionalized (polymers have reactive terminal groups such as carboxylic acids or amines) and therefore they are easily targeted to certain tissues or organs. Moreover, given the high (and modulable) biodegradability of certain polymers such as poly(lactic acid) (PLA) or poly(lactic-co-glycolic) acid (PLGA) the rate of drug release can be easily controlled.

This work focuses on the preparation and characterization of polymer nanoparticles made of ethylcellulose and PLGA from template nano-emulsions. By the incorporation of a cationic surfactant in the formulation, positive surface charges were attained. Positively charged nanoparticles allow for strong electrostatic interactions with anionic molecules such as proteins, which could be interesting for the design of targeted and controlled drug release systems.

Nano-emulsions were prepared by the PIC method using two slightly different techniques and were characterized by DLS (dynamic light scattering) and light transmittance versus time experiments.

Nanoparticles were prepared by solvent evaporation and were characterized by DLS and Z-potential measurements. Their interaction with seroalbumin, the major protein in blood, was also studied through DLS and Z-potential measurements.

Keywords: cationic nanoparticles, cationic nano-emulsions, polymers, controlled release, targeted release, seroalbumin, Z-potential, dynamic light scattering.

2. RESUM

Actualment, un gran esforç en recerca farmacèutica es dedica a la investigació de sistemes d'alliberament controlat de fàrmacs. Una de les opcions més innovadores és l'ús de nanopartícules com a vectors no virals per l'alliberament controlat i/o dirigit de fàrmacs a òrgans o teixits diana. En aquests camps, les nanopartícules més usades són les polimèriques donada la seva versatilitat: poden funcionalitzar-se fàcilment gràcies als grups químics reactius que contenen els polímers (àcids carboxílics, amines…) per dirigir-les a la seva diana. A més, donada l'alta (i modulable) biodegradabilitat d'alguns polímers com l'àcid polilàctic (PLA) o l'àcid poli(làctic-co-glicòlic) (PLGA) permeten l'alliberament gradual dels fàrmacs quan les partícules assoleixen la seva diana.

Aquest treball es basa en la preparació i caracterització de nanopartícules polimèriques d'etilcel·lulosa i PLGA a partir de nano-emulsions plantilla. Amb la incorporació d'un tensioactiu catiònic a la formulació s'aconsegueixen càrregues superficials positives que permeten una forta interacció amb biomolècules aniòniques com les proteïnes, que podria ser d'interès quan es dissenyen sistemes d'alliberament dirigit de fàrmacs.

Les nano-emulsions s'han preparat pel mètode PIC amb dues tècniques lleugerament diferents i s'han caracteritzat per DLS (dynamic light scattering) i per experiments de transmitància versus temps.

Les nano-partícules s'han preparat per evaporació del dissolvent i s'han caracteritzat per DLS i potencial-Z. La seva interacció amb seroalbúmina, la proteïna majoritària a la sang, també s'ha determinat a través de mesures de DLS i de potencial-Z.

Paraules clau: nanopartícules catiòniques, nano-emulsions catiòniques, polímers, alliberament controlat, alliberament dirigit, seroalbúmina, potencial-Z, dynamic light scattering.

3. INTRODUCTION

Systems constituted by nanometric entities often have peculiar properties that differentiate them from their micrometric equivalents due to their higher surface-to-volume ratio. These properties give rise to an infinity of applications.

3.1. NANO-EMULSIONS

Nano-emulsions are colloidal dispersions of liquid droplets in a liquid media with a submicrometric droplet size. A nano-emulsion is composed of the same constituents as any other emulsion: an aqueous and an oily phase that can form oil-in-water (O/W) or water-in-oil (W/O) emulsions. The use with of a third element that reduces the surface tension, a surfactant, can be necessary in some cases.

The border between nano- and micrometrically-sized emulsions is diffuse, but a radius of 500 nm is often accepted as the upper limit in size for nano-emulsions [1].

3.1.1. Nano-emulsion stability

Unlike micrometrically-sized emulsions, nano-emulsions are thermodynamically unstable but may show a high kinetic stability [1]. Such thermodynamic instability can easily be understood by the Gibbs free energy of emulsion formation in equation 1 that can be applied to any colloidal system:

$$\Delta G_f = \gamma_{w\text{-}o} \cdot \Delta A_f - T \cdot \Delta S_f \quad (1)$$

Where ΔG_f is the increment of the Gibbs free energy of the emulsion formation, $\gamma_{w\text{-}o}$ is the surface tension between the water (w) and oil (o) phase, ΔA_f is the increment of interfacial area, T is the absolute temperature, and ΔS_f is the entropy increment for the emulsion formation.

The Gibbs free energy of a micrometrically-sized emulsion formation is negative, and therefore it is thermodynamically stable. On the other hand, even with the addition of a surfactant (which can be either ionic or non-ionic) a nano-emulsion's Gibbs free energy of

formation is positive due to the much larger increase in surface area. Due to its thermodynamic instability, the system will need an external energy input to form and will have a strong tendency to reduce its surface area by increasing the droplet size in order to achieve a stable state. This increase in size could be attained by flocculation and coalescence (leading to sedimentation or creaming), but such phenomena are greatly disfavoured due to the high specific surface area that these systems possess. The primary destabilization mechanism for a nano-emulsion is the Ostwald ripening, which consists of a mass transfer from the smaller droplets to the larger ones through the continuous phase due to their different chemical potentials [1]. If larger droplets increase enough in size before chemical equilibrium is reached, the kinetic stability of the system will be diminished, and coalescence and other phenomena could occur. Therefore, it can be concluded that emulsions with greater stability are those that have a highly uniform droplet size (low polydispersity) and in which the dispersed phase components are completely insoluble in the continuous phase.

3.1.2. Preparation of nano-emulsions

Nano-emulsions can be prepared using either high or low energy methods. High-energy methods rely on intimate mixture of the emulsion components through vigorous agitation, sonication or high-pressure homogenization to achieve emulsification. Since only a very small fraction of the energy consumed is actually used to produce emulsification, these methods imply a high energy consumption. In addition to that, high-energy emulsification often yields large and polydisperse droplet sizes, which is highly undesirable since it favours Ostwald ripening.

Low-energy emulsification methods have none of these disadvantages: they generally produce small droplet sizes with low polydispersity at a very low energy consumption. Low-energy methods can be classified into two main groups: phase inversion and non-phase inversion methods depending the presence or the absence of a spontaneous curvature change. In either case, only simple stirring is needed to perform the emulsification [2].

Non-phase inversion emulsification is based on the use of a three-component homogeneous system as a precursor to the nano-emulsion. The phenomena in which this method based is called the “Ouzo” effect, named after the Greek beverage “Ouzo” that can be prepared thanks to the so-called effect [3]. In the preparation of this liquor, a homogeneous system consisting of ethanol, water and small amounts of an anise-flavoured oil (mainly p-propenylanisole) is diluted with water. In the water enriched system that is formed, the oil

solubility is drastically reduced and small oil droplets with high kinetic stability are formed. The use of this method is limited by the small concentration of solute that can be incorporated to achieve a nano-emulsion state, which in turn yields a very small amount of nano-emulsion compared to the large quantity of solvents used in the process.

On the other hand, phase inversion emulsification makes use of the chemical energy released by a phase transition that happens during the generation of the emulsion [2]. This phase transitions can be promoted by a change in temperature at constant composition (phase inversion temperature, PIT, method) or by a change in composition at constant temperature (phase inversion composition, PIC, method). Regardless of the method used, it is essential for the system to go through a phase with no curvature to reach a final nano-emulsion state. This zero curvature phases are bicontinuous structures (bilayers) or lamellar liquid crystal phases (bilayers separated by a layer of the continuous phase) [2].

To prepare nanoemulsions by the PIT method, the starting material is a system at its phase transition temperature that has its hydrophilic and lipophilic properties perfectly balanced, and consequently it has no spontaneous curvature. These systems must be formulated using a surfactant with a greatly temperature dependent hydrophilic-lipophilic balance [2]. If the mixture is cooled or heated an O/W or a W/O nano-emulsion will respectively form.

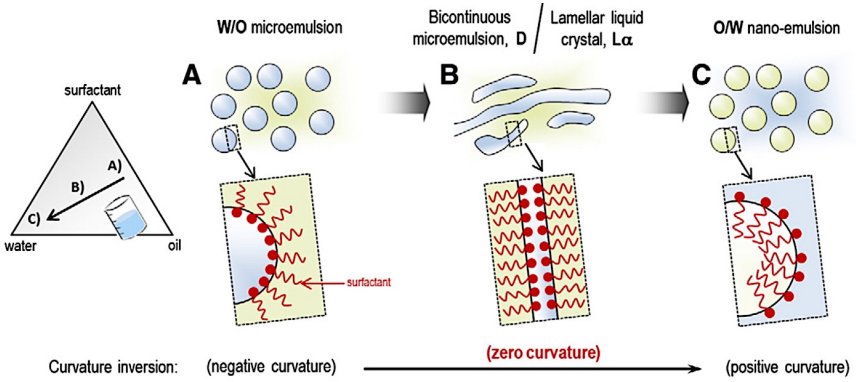

Figure 1. Schematic representation of the changes in curvature during a PIC method synthesis. From reference 2

In nano-emulsions prepared by the PIC method, a third component is added to a homogeneous mixture of the other two. This third component changes the composition of the system and, if it is properly selected, the latter will undergo a phase inversion [1,4]. For example,

to obtain an O/W nano-emulsion, an aqueous component is gradually added to a mixture of surfactant and oily phase. In this case, the system first forms a W/O nano-emulsion that finally reverts to an O/W one by going through lamellar liquid crystals or bicontinuous phases. The presence of salts greatly affects this phase transitions will be further discussed in this work [5, 6].

3.1.3. Nano-emulsion applications

Nano-emulsions find their major application in pharmacology and cosmetics [3, 7, 13]. In these fields, nano-emulsions are used over micrometrically-sized emulsions due to their high kinetic stability and the lower surfactant concentration needed to obtain them. Research is primarily focused on the encapsulation of lipophilic substances in hydrophilic micellar containers to improve their absorption and transport [7]. One of their major applications, currently being researched, is their use for nanoparticle preparation [9]. It must be emphasized that high energy methods are still predominant industrially but the transition to low energy methods, mainly the PIC method, is taking place quickly due to their substantially lower energy consumption.

3.2. NANOPARTICLES

Nanoparticles are defined as solid entities of any morphology with sizes ranging from 1 to 100 nm [10]. The upper limit is fixed so that the particles show a great variation of their properties depending on size. Nanoparticles with sizes greater than 100 nm still show enhanced surface properties over micro-particles, but they are no longer strongly related to the particle's radius. Unlike emulsions, nanoparticles are solid-based systems that may exhibit high morphologic rigidity and an even higher stability level given that particles cannot experience Ostwald's ripening. A great variety of different kinds of nanoparticles can be obtained depending on the material used: metallic, ceramic or polymer-based nanoparticles are the most usual, but protein or lipid-based nanoparticles are also systems to be considered. This work will focus on the synthesis of polymer-based nanoparticles using nano-emulsions as templates.

3.2.1. Polymer nanoparticle synthesis from nano-emulsions

Producing nanoparticles (solid spheres) made of polymers from nano-emulsions is an easy and reproducible procedure once the system has been properly tuned. Note that a top-down milling approximation is not possible for polymer or biomolecule-based particles due to their

poor mechanical properties, namely, high elasticity and plasticity due to their low melting temperature.

There are two ways of synthesizing polymer nanoparticles using nano-emulsions as templates. The first one is based on polymerization in nano-emulsions. The monomer or monomers (the oily components of the system) are dispersed in an aqueous media with the aid of a surfactant. The polymerization is then started by the addition of an initiator to the aqueous phase or by other means such as UV light or enzymes [1]. The final product is a dispersion of polymer nanoparticles that usually contains initiators and/or other unwanted subproducts which must be removed of the system by means of dialysis or other methods [1,11].

Nanoparticle synthesis based on the use of a preformed (prepolymerized) polymer takes place by emulsification of an oily phase (containing the polymer in solution) in an aqueous phase with the aid of a surfactant or a mixture of surfactants. Once the emulsion has been formed, solvent must be removed from the droplets in order to obtain solid polymer nanoparticles. This can be achieved by evaporation of the solvent at atmospheric pressure [9] or with the aid of vacuum [6]. If the solvent presents partial solubility in the continuous phase it can also be extracted by dilution of the continuous phase. The result is an aqueous dispersion of polymeric nanoparticles stabilized by the surfactant that can have a particle sizes as small as 10 nm and a low polydispersity [6,12].

3.2.2. Nanoparticle properties and applications

Nanoparticles can show a high stability. They can be more stable than nano-emulsions due to the fact that they are solid and therefore, destabilization through Oswald's ripening cannot not occur. Since nanoparticles can have a density greater than the emulsion droplets from which they were prepared, in some cases, sedimentation and creaming processes may be faster than in nano-emulsions. Nanoparticles find their application in very divergent fields. For example, silver nanoparticles are used in antimicrobial fabrics, ceramic nanoparticles are key to industrial catalysers and metal oxides nanoparticles have been used for centuries in steel hardening and glass staining.

On the other hand, polymeric nanoparticles applications are more recent [13], and are generally based on lipophilic drug carrying and targeted release through surface functionalization. These drugs or biomolecules can be either dispersed within a biodegradable

polymer or be contained in nano-capsules. In these fields, in which nanoparticles are usually administered via parenteral injections, interaction with major blood components, namely blood proteins, must be considered. Protein absorption is the first phenomena that takes place when nanoparticles enter the bloodstream. Blood contains a concentration of proteins of up to 84 g/L of which, at least 40 g/L correspond to serum albumin. Since general immune response is triggered by protein adsorption, the specific composition of the adsorbed protein layer creates a molecular signature that determines the nanoparticles fate in the body (rate and route of clearance, toxicity, etc.). Due to nanoparticles high specific surface area, this adsorption process (called opsonization) is even more relevant that in the case of micrometrically sized particles. Since some blood proteins are above their isoelectric point (negative net charge), a positive particle surface charge can also accentuate this process[14].

So, as a summary, this work will focus on preparation and characterization of cationic nanoparticles from template nano-emulsions (prepared by the PIC method) and the study of their interaction with seroalbumin, the major protein present in blood.

4. OBJECTIVES

The aim of this work is to design cationic polymeric nanoparticles made from template nano-emulsions obtained by the phase inversion composition method for pharmaceutical applications. To attain the main objective the following particular objectives are proposed:

1) Preparation of cationic nano-emulsions by the PIC method and their characterization.

2) Preparation of cationic polymer nanoparticles from template nano-emulsions and their characterization.

3) Study of the interaction of the cationic nanoparticles with seroalbumin.

5. EXPERIMENTAL SECTION

5.1. MATERIALS

In this section, the materials used will be briefly described. A more complete and referenced description (including biocompatibility data) can be found in the annex 1.

5.1.1. Surfactants

Chemical Family (type)	Comercial name (supplier, purity)	Chemical Name	HLB
Polyglyceryl fatty acid esters (non-ionic)	Cithrol PG 3PR-LQRB (Croda, *)	Polyglyceryl-3 ricinoleate	3.4[c]
Polyoxyethylene fatty alcohol ethers (non-ionic)	Brij 92V (Fluka, *)	Polyoxyethylene oleyl ether	4.9[c]
Polyoxyethylene fatty acid esters (non-ionic)	Cremophor EL (BASF, *)	PEG-35 castor oil glycerides	13[b]
	SP Glicerox 767HC (Croda, *)	PEG-6 caprylic and capric glycerides	13.2[c]
	Cremophor RH455 (BASF, *)	Mixture of PEG-40 and 5% propylene glycol	14[b]
Polysorbates (non-ionic)	Tween 21 (Croda, *)	PEG-4 sorbitan monolaurate	13.3[a]
	Tween 85 (Croda, *)	PEG-20 sorbitan trioleate	13.3[a]
	Tween 80 (Croda, *)	PEG-20 sorbitan monooleate	15.0[a]
	Tween 20 (Croda, *)	PEG-20 sorbitan monolaurate	16.7[a]
Quaternary Amidoamine (cationic)	Varisoft RTM 50 (Evonik, 40% in H_2O)	Ricinoleamidopropyltrimonium methosulfate	-

(*) Products can be considered ~100% active matter (no information about purity was present in any datasheet).
(a) From Croda Home Care product datapage. **(b)** From BASF Care Creations datapage. **(c)** From original container label.

Table 1. Surfactants used in this work.

5.1.2. Polymers

Chemical name	Supplier	Commercial name	MW[a] [g/mol]
Poly(D,L-lactide-co-glicolide) acid (PLGA)	Evonik Rohm GmbH	Resomer RG752H	4000 - 15000
Ethylcellulose (EC)	Dow Chemicals	Ethocell Standard 10 Premium	~65000

(a) Abreviation for molecular weight. From manufacturer data, determined by viscosimetry.

Table 2. Essential information about the polymers used in the present work

5.1.3 Solvents and aqueous components

Chemical name	Supplier	Purity [%]	Boiling point [ºC]	Solubility in H_2O [%w]
Ethyl acetate	Merck	≥99.8	77	7.39

Table 3. Description of ethyl acetate's most relevant properties.

Chemical name	Supplier	Purity [%]	Common name	pH	C [mM]
N-(2-hydroxyethyl)piperazine-1-ethanesulfonic acid	Sigma	≥99.5	HEPES	7.4 (25ºC)	20
Tris(hidroxymethyl)-aminomethane	Sigma	≥99.9	TRIS, Trometamine	7.4 (37ºC)	50
Phosphate buffered saline	Sigma	≥99.5[a]	PBS	7.4 (25ºC)	160

(a) Purity of the least pure reagent used for preparation of PBS. All reagents were at least analytical reagent grade.

Table 4. Aqueous phases used in the development of this work. More information can be found in annex 1.

5.1.4. Biomolecules

Biomolecule type	Supplier	Purity [%]	Common name	pI	Solubility [g/L]
Protein	Sigma	≥98	Bovine Serum Albumin (BSA)	4.7	>80 (H_2O, 37ºC)[26]

Table 5. Description of bovine serum albumin's most relevant properties. Further description can be found in annex 1

5.2. EQUIPMENT

5.2.1. Photon correlation spectrometer

Dynamic light scattering was used for measuring particle and droplet sizes. This technique is based on the Brownian motion of particles. A laser is focused on the sample and the amount of light scattered is measured. The amount of light scattered fluctuates slightly over time due to the Brownian motion of the dispersed entities. From that fluctuations, a diffusion coefficient can be calculated by the Stokes-Einstein equation [15]:

$$D = \frac{k_b T}{6\pi \eta R_H} \quad (2)$$

Where k_b is Boltzmann's constant, T the temperature, η the viscosity of the continuous media and R_H is the mean hydrodynamic radius of the particles. The hydrodynamic radius is the apparent size of particles in solution, that is, with their solvation spheres. So, if particles are not spherical or have molecules adsorbed onto them, the hydrodynamic radius will be the radius of the ideal sphere that would diffuse at the same rate as the particles being measured.

To avoid multiple scattering signals, a 3D photon correlation spectrometer (3D-PCS) equipped with two lasers beams was used. By comparing the scattering rate of the two lasers, multiple scattering signals can be suppressed.

For this work, an LS-Instruments 3D-PCS was used to determine particle and droplet sizes and polydispersity. The instrument uses a red He-Ne laser with a wavelength of 633 nm. During the measurements, samples were kept at 25ºC in a decalin (decahydronaphthalene) bath.

5.2.2. Turbiscan

A Turbiscan Lab instrument from Formulaction (Toulouse, France) was used to perform long-term stability measurements. This equipment measures transmittance and light backscattering of the sample in the near infrared (λ = 880 nm) across all its height several times during a user-defined time interval. For this work, a transmittance and backscattering analysis every hour for 24 hours was performed. This frequency and analysis length allows for detection of the destabilization mechanism (creaming or sedimentation) even for the most stable systems prepared.

5.2.3. Zetasizer

A Zetasizer Nano Z instrument from Malvern Instruments Ltd. (Malvern, United Kingdom) was used to measure ζ-potential (Z-potential) of nanoparticles dispersions. ζ-potential can be thought of as the effective surface charge of particles. Any particle in suspension is surrounded by ions of the opposite charge. These ions arrange in a bilayered fashion creating what it is called the electrical double layer. The first layer is composed of strongly attached ions and it is called the Stern Layer. In the second layer, ions are not so strongly attached, and two regions can be distinguished: the first one, closer to the particle core, is composed of ions that are attached to the particle with enough force to follow its Brownian movement. The second region contains ions that are weakly bound and cannot follow the particle's movement. The ζ -potential is the electrical potential at the border between these two regions (relative to a point in the bulk liquid media away from the particle's interface).

The Zetasizer Nano Z instrument calculates the ζ-potential applying an electrical potential of about 150V and optically measuring the speed at which the charged particles travel (electrophoretic mobility). Z-potential is then calculated by the Henry equation:

$$\mu = \frac{2\,\varepsilon\,Z\,f(kr)}{3\,\eta} \tag{3}$$

Where, μ is the electrophoretic mobility, ε is the electric permittivity of the surrounding media, Z is the ζ-potential, η is the viscosity of the medium and f(kr) is the Henry function. This function can be 1.5 for diluted aqueous media (like in this work) or 1 if the media has low permittivity (like organic solvents) [16].

5.2.4. Other equipment

Mixer

A Vortex-Genie 2 (Scientific industries) mixer was used at maximum vortexing speed (2700 RPM) in order to ensure proper mixing during nano-emulsion preparation by the PIC method.

Rotary Evaporator

Rotavapor® R-210/215 from BUCHI Labortechnik AG was used to prepare nanoparticles form nano-emulsions. The rotation speed can be adjusted from 20 to 280 RPM and the heating bath from +20ºC to +180ºC (temperatures greater than 80ºC require the use of thermal oils).

Analytical Balance

The weight of all chemicals was determined by using an AB204S/FACT analytical balance from Mettler Toledo. The balance has a maximum capacity of 220 grams and a precision of 0.1 mg.

5.3. METHODS

5.3.1. Nano-emulsion preparation by the phase inversion composition method

Nano-emulsions were prepared in 4-gram batches by the PIC method through two different techniques. Preparation by method 1 consisted on weighting the required amount of aqueous phase with a syringe and slowly adding it over the previously mixed oily and surfactant phases on continuous stirring. The surfactant phase contained all surfactants needed.

On the other hand, preparing nano-emulsions by method 2, consisted on using an aqueous phase that already contained the required amount of the cationic surfactant Varisoft RTM 50 (Cat A) and slowly adding it over an intimate mixture of the oily phase and the other surfactant. (only binary mixtures of surfactants were used on the development of this work).

5.3.2. Nano-emulsion formation determination

Since nano-emulsions exhibit high transmittance and a characteristic red and/or blue shine, nano-emulsion formation was first visually determined. In the following Figure, several examples of nano-emulsion appearance can be found.

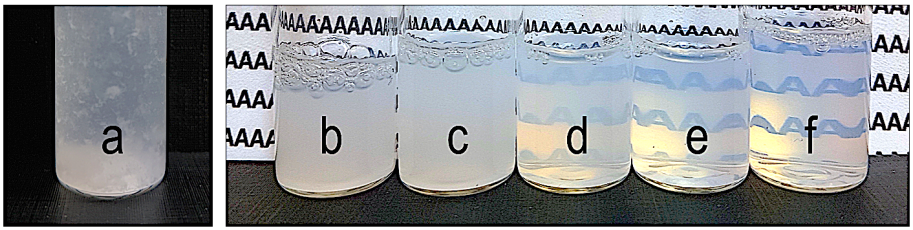

Figure 2. Nano-emulsions ranging from red/blue and transparent (f) indicating nano-emulsion formation to completely destabilized (a) indicating total phase separation. The limit for nano-emulsion formation domain was set for nanoemulsions similar to b and c (emulsions with droplet radii > 250 nm).

5.3.3. Nanoparticle preparation from template nano-emulsions

Polymeric nanoparticles were prepared by evaporation of the organic solvent from O/W nano-emulsions in a rotary evaporator at 25ºC, 43 mbar and 150 RPM for 45 minutes. By using these conditions, an ethyl acetate concentration lower than 5000 ppm is ensured [17]. At the end of the evaporation, all lost mass was replaced with Milli-Q water to keep osmolarity constant.

5.3.4. Droplet or particle size determination

Particle or droplet size was determined by dynamic light scattering (DLS) in a 3D-PCS at 25ºC (section 5.2.1). Samples were measured undiluted when possible. If samples were too opaque to be directly measured, a dilution of 100 µg in 1g of final mass were performed with Milli-Q water.

5.3.5. Z-potential determination

ζ-potential measurements were performed in a Zetasizer Nano Z instrument (section 5.2.3). Samples were diluted to meet conductivity requirements in a 1 to 20 ratio (100 µg of sample in 2g of total mass) with Milli-Q water. Measurements were triplicates, each one consisting of 20 scans. Disposable 1 mL Malvern polycarbonate measurement cells were used.

5.3.6 Interaction with bovine serum albumin

Interaction of positively charged nanoparticles was characterized by Z-potential and by complex hydrodynamic radius. As Vittazz [18] described, samples containing 1000 cm^2 of nanoparticles (calculated by the expression 4) were incubated with different concentrations of seroalbumin for 10 minutes at 37ºC. Samples were then diluted to 2 grams of total mass and Z-potential and hydrodynamic radius was determined as described in previous sections.

$$S = n4\pi r^2 = 3\frac{V}{r} = 3\frac{m}{r\rho} \quad (4)$$

Where S is the particle surface n is the number of nanoparticles, r is the radius of particles, V is the volume of the particles, m the mass of polymer and ρ its density.

5.3.7 Stability and destabilization mechanism determination

Sedimentation or creaming, was determined visually and by transmittance versus sample height versus time Turbiscan experiments. From the latter, apparent destabilization kinetic constants (destabilization indexes) were also calculated.

6. RESULTS AND DISCUSSION

6.1. SYSTEMS BASED ON ETHYLCELLULOSE AS THE POLYMER

6.1.1 Formation and characterization of nano-emulsions

The formation of nano-emulsions in the [aqueous phase / CatA:CEL / 6% EC in ethyl acetate] at 25ºC system was studied using diluted PBS and TRIS buffer solutions as the aqueous phase. This system had already been studied in the past by using water, 0.16M PBS and HEPES as the aqueous component [19]. It was found that stable nano-emulsions were formed using water or an HEPES buffer. However, when 0.16M PBS was used as the aqueous phase, only low stability systems were formed. In the present work it is intended to explore the influence of the electrolyte concentration in the stability of the nano-emulsions of the [PBS / CatA:CEL / 6% EC in ethyl acetate] at 25ºC system as well as the use of other aqueous components. Previous research performed on similar PLGA-based systems showed a great impact of the aqueous phase concentration and composition in the formation and characteristics of the nano-emulsions [6]. For screening purposes, a system consisting of a binary mixture of CatA and CEL (CatA:CEL = 1:1) and an oil-to-surfactant ratio (O/S) of 70:30 was chosen based on the previous results reported by Leitner et al [19] (if not otherwise stated, the O/S ratio used in this whole work is 70/30). Water content was 90% and 95%, and polymer concentration was 6% w/w in ethyl acetate. Formation of nano-emulsions at 25ºC was performed by the two methods explained in section 5.3.1. As shown in Table 6, no stable emulsions could be prepared by using only water as the aqueous phase in contrast to the findings of Leitner et al [19]. However, nano-emulsions with droplet sizes lower than 100 nm formed with PBS at different concentrations and TRIS buffer as the aqueous phase.

The nano-emulsions of the [PBS / CatA:CEL / EC 6% in ethyl acetate] systems were further characterized at 25ºC using different concentrations of phosphate buffered saline and method 1 of preparation. Emulsions prepared at 95% aqueous phase had smaller droplet sizes than the ones prepared at 90% (Figure 3). This trend can be explained from a solvent diffusion standpoint: in systems containing 95% of water, more ethyl acetate can diffuse from the droplets to the continuous phase before saturation, and therefore, smaller droplets are obtained [6]. Due to their larger hydrodynamic droplet sizes, research on 90% PBS systems was discontinued. As shown in Figure 3, hydrodynamic radius decreased when increasing the PBS concentration up

to a concentration of 0.08M. This can be explained from an osmotic approach: solutes, even non-electrolytic ones, can force more solvent out of the micelles than pure water by increasing the osmotic pressure of the continuous media. This reduces droplet size and, therefore increases kinetic stability of nano-emulsions [5,6]. For higher concentrations of PBS, the hydrodynamic radii kept approximately constant around 70 nm. The stabilization in size at PBS concentrations higher than 0.08M could be caused by depletion of extractable solvent from the droplets.

[Aqueous phase / CatA:CEL / EC 6% in ethyl acetate] at 25ºC

Aqueous phase	Preparation method	Nano-emulsion formation	Droplet size {nm}
PBS (variable concentration)	Method 1	Yes	62.2± 0.9 (0.10M)
	Method 2	Yes	65±1 (0.1333 M)
TRIS 0.05 M[a]	Method 1	Yes	89±1
	Method 2	Yes	76±1
Milli-Q water	Method 1	No	-
	Method 2	No	-

(a) Cationic surfactant content higher and lower than CatA:CEL = 1:1 have been successfully essayed (see Figure 12)

Table 6. Summary of nano-emulsion formation and droplet size in essayed systems containing ethylcellulose as the polymer

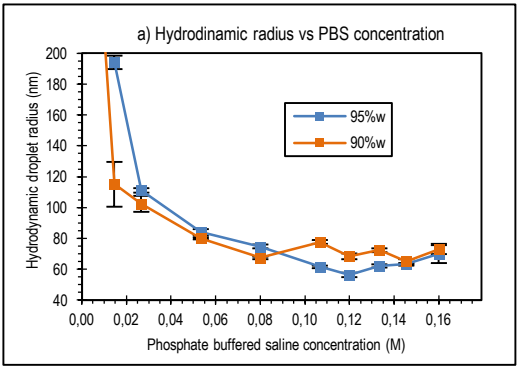

Figure 3. Hydrodynamic radius variation with PBS concentration of nano-emulsions in the [PBS / CatA:CEL / EC 6% in ethyl acetate] systems at 25ºC with an O/S ratio of 70/30 and 90% or 95% aqueous component.

All studied nano-emulsions showed destabilization by sedimentation several days after preparation (Figure 4a). Stability was assessed by light transmittance and backscattering experiments. As shown in Figure 4, transmittance increased uniformly over the lower and central region of the sample, which could be caused by droplet shrinkage due to solvent diffusion from the droplets to the continuous media during the measurement period. The sharp transmittance peak appearing in the upper part of the sample is due to the sedimentation of the dispersed droplets.

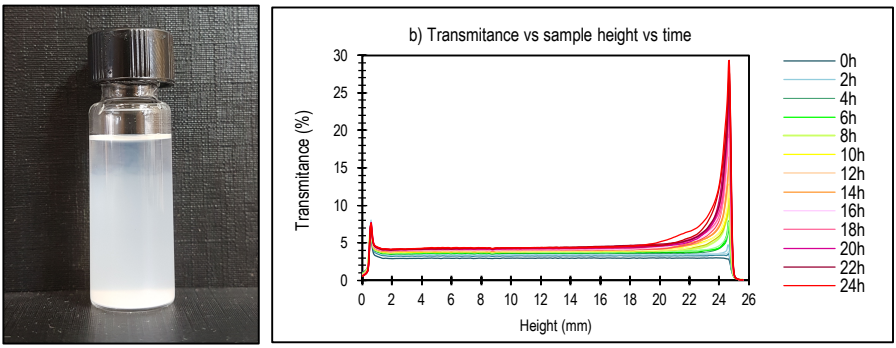

Figure 4. a) Visual aspect of a sedimented nano-emulsion after 5 days of storage at 25ºC. b) Light transmission as a function of sample height and time of a nano-emulsion in the [PBS 0.016M / CatA:CEL / EC 6% in ethyl acetate] system with O/S=70/30 and 95% PBS at 25ºC.

The destabilization index determined from light transmission spectra reveal that stability is maximum for a concentration of PBS of 0.08M (Figure 5). Since, 0.08M is the PBS concentration from which droplet sizes do not further reduce by increasing PBS concentrations, the decrease in stability for PBS concentrations higher than 0.08M could be due to the shielding effect of phosphate ions on positive surface charge of the droplets, reducing electrostatic repulsion between them. The lower stability of the system with the lowest PBS concentration (0.016M) could be due to its higher droplet sizes. As it can be seen from the Stokes equation for terminal velocity of a falling sphere (equation 5), particles with a greater size could sediment faster (considering that the aqueous phase density and viscosity remains constant when changing PBS concentration):

$$v = \frac{2}{9}\frac{(\rho_d - \rho_m)}{\eta} g\, r^2 \qquad (5)$$

Where v is the settling speed, ρ_d and ρ_m are the densities of the dispersed phase and the media, η is the viscosity of the media, g is gravity's acceleration and r is the radius of the spherical particle.

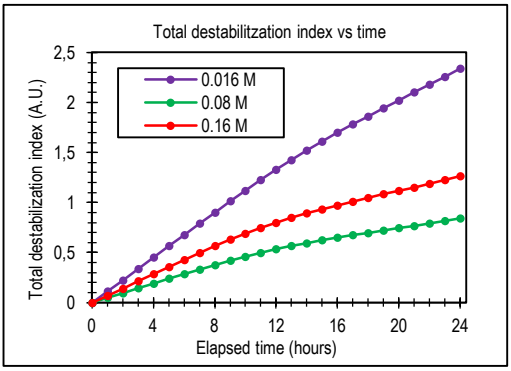

Figure 5. Total destabilization index versus time for [PBS / CatA:CEL / 6% EC in ethyl acetate] systems with different PBS concentrations at 25ºC.

Concerning ethylcellulose-based nano-emulsions prepared using TRIS as the aqueous phase, hydrodynamic droplet sizes and long-term stability were characterized as a function of the cationic surfactant content on the [TRIS / CatA:CEL / EC 6% in ethyl acetate] system with 95% TRIS content at 25ºC. As shown in Figure 6a, hydrodynamic radius increased with the cationic surfactant content of the system. This could be due to the HLB of the surfactant mixture being higher than required to prepare O/W nano-emulsions. As for the previous system, larger droplet sizes also implied higher sedimentation rates leading to a poorer long-term stability (Figure 6b). All samples sedimented after several days at 25ºC. Light transmission spectra were similar to that shown in Figure 4b.

When compared to nano-emulsions with PBS, nano-emulsions with TRIS showed higher droplet sizes (Figure 6a) and a lower long-term stability (Figure 6b). In systems containing Milli-Q water, where stabilizing osmotic effects are less intense due to de absence of solutes, nano-emulsions did not form at any of the essayed compositions.

From the present data it can be inferred, that a certain concentration of solutes, either electrolytic or non-electrolytic, may be necessary in order to obtain stable nano-emulsions in these systems. For this reason, ethyl cellulose-based systems using TRIS or PBS as the aqueous phase were selected for the preparation of nanoparticles.

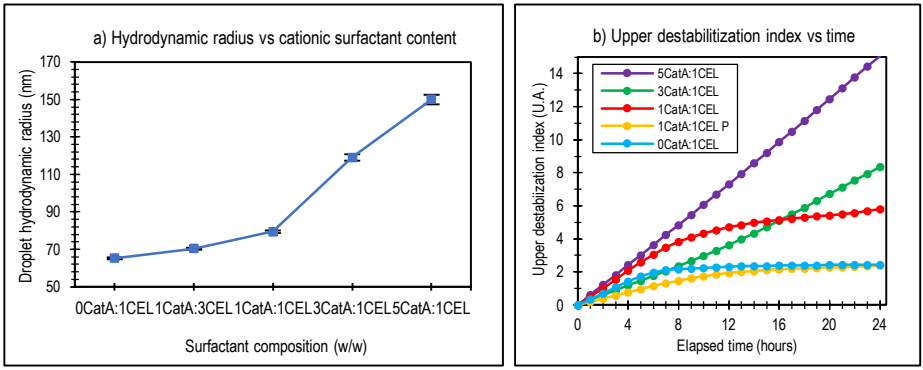

Figure 6. a) Droplet size versus CatA content for nano-emulsions in the [TRIS / CatA:CEL / EC 6% in ethyl acetate] system prepared by method 2 with 95% TRIS at 25ºC. b) Long-term stability kinetics for the same systems as in Figure 6a. The [PBS 0.08M / CatA:CEL / EC 6% in ethyl acetate] system with 95% PBS at 25ºC is included as "CatA:CEL P" for comparison.

6.1.2. Formation and characterization of nanoparticles

Nanoparticles in the [PBS / CatA:CEL / EC 6% in ethyl acetate] system were prepared from template nano-emulsions at 25ºC as described in section 5.3.3. PBS content was fixed at 95% w/w. Particle size, Z-potential and long-term stability was characterized as a function of the PBS concentration.

Particle size followed a similar trend as the droplet size of the template nano-emulsions from which nanoparticles were prepared. There was a decrease in particle size for increasing PBS concentrations up to a concentration of 0.08M (Figure 7). Since solvent is extracted during nanoparticle preparation, nanoparticle radius was smaller when compared with their template nano-emulsions.

Stability against sedimentation was visually assessed and was greater than 1 week for all studied nanoparticle dispersions. For systems with a PBS concentration of 0.08M sedimentation occurred after more than one month from preparation.

Due to the presence of the cationic surfactant CatA, the surface charge of the nanoparticles was positive. As it can be seen in Figure 7, ζ-potential decreases (becomes less positive) as the buffer solution concentration is increased. This is attributed to a shielding effect of phosphate ions.

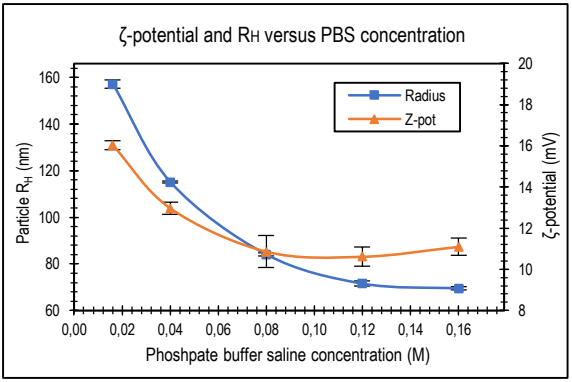

Figure 7. Particle size vs PBS concentration in the [PBS / CatA:CEL / EC 6% in ethyl acetate] systems with 95% PBS at 25ºC. Nanoparticle's ζ-potential as function of PBS concentration for the same system is also displayed.

Nano-particles in the [TRIS / CatA:CEL / EC 6% in ethyl acetate] with 95% TRIS were also prepared at 25ºC from their template nano-emulsions as described in section 5.3.3. Particle size, ζ-potential and long-term stability were characterized as a function of the cationic surfactant content. A higher cationic surfactant content lead to larger particle sizes, which could be explained by the same effects as in equivalent nano-emulsion systems in section 6.1.1. (Figure 8). Regarding ζ-potential dependence with cationic surfactant content, it can be inferred that a higher cationic surfactant content, implies a greater amount of positively charged surfactant ions on the surface of droplets which leads to a higher surface charge (Figure 8). A greater particle size has been related to lower stability (possibly explained by equation 5), with samples suffering sedimentation in 1 (CatA:CEL=5:1) to 5 days (CatA:CEL=1:1). Lower cationic surfactant contents lead to sedimentation times exceeding 1 week.

TRIS buffer provided a significant stabilizing effect at a concentration of 0.05M, while not strongly shielding the surface charge. This can be attributed to its weak electrolytic character. As for the higher particle size and poorer stability obtained with nanoparticle dispersions of TRIS-based systems versus those prepared with PBS, it may also be attributed to the weaker stabilizing effect of TRIS due to its lower concentration and weak electrolytic character.

Ethylcellulose-based systems using TRIS as the aqueous phase were chosen to essay their interaction with seroalbumin at surfactant compositions of CatA: CEL = 1:1 and 1:3 due to their relatively high ζ-potential and suitable stability.

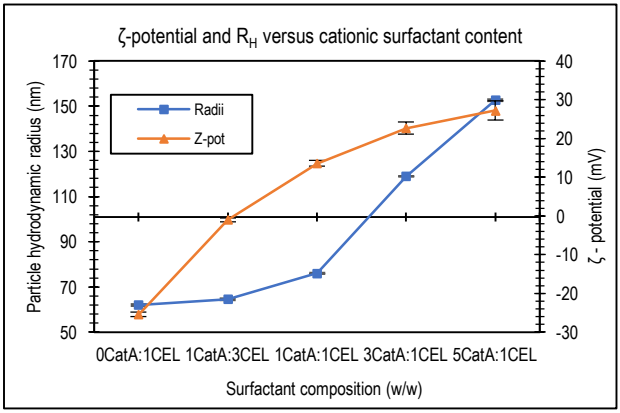

Figure 8. Particle size versus cationic surfactant content for the [TRIS / CatA:CEL / EC 6% in ethyl acetate] systems with 95% TRIS at 25ºC.

6.2. SYSTEMS WITH PLGA AS THE POLYMER

6.2.1. Formation and characterization of nano-emulsions

The formation of cationic nano-emulsions was studied in the [aqueous component / CatA : non-ionic surfactant / 6% PLGA in ethyl acetate] systems at 25ºC. If not otherwise stated, the oil-to-surfactant ratio was fixed at 70/30. A broad screening of systems containing different aqueous phases and different surfactants was performed. At first, 0.16M phosphate buffered saline was used as the aqueous component and several non-ionic surfactants (NIS) were combined with the cationic surfactant Varisoft RTM 50 (Cat A). Table 7 summarizes the main results obtained. From the two systems that formed nano-emulsions it can be inferred that cosurfactant HLB needed in order to disperse the polymer solution in an aqueous media could be about 13.

Other aqueous phases were essayed with a narrower selection of the previously used surfactants (Table 8). No nano-emulsions were formed when using HEPES or 0.08M PBS as the aqueous phase. When using water, nano-emulsions were formed with Cremophor EL, but nano-emulsions prepared with the same surfactant and TRIS as the aqueous component showed higher transparency and a more intense blue shine.

During the screening process, PLGA concentrations of 4% w/w in ethyl acetate were also essayed leading to slightly lower droplet sizes and enhanced stability. To keep systems

comparable with EC-based systems PLGA concentration used on further studies was kept at 6% w/w.

[0.16 M PBS / CatA : NIS / PLGA 6% in ethyl acetate].

Surfactant's Chemical Family	Surfactant's Comercial Name	Surfactant's Chemical name	NIS' HLB	Nano-emulsion formation
Polyglyceryl fatty acid esters	Cithrol PG 3PR-LQRB	Polyglyceryl-3 ricinoleate	3.4	No
Polyoxyethylene fatty alcohols	Brij 92V	Polioxyethylene oleyl ether	4.9	No
Polyoxyethylene fatty acid esters	Cremophor EL	PEG-35 castor oil glycerides	13	Yes[a]
	SP Glicerox 767HC	PEG-6 caprylic and capric glycerides	13,2	No
	Cremophor RH455	Mixture of PEG-40 and 5% propylene glycol	14	No
Polysorbates (ethoxylated sorbitan fatty acid esters)	Tween 21	PEG-4 sorbitan monolaurate	13.3	No
	Tween 85	PEG-20 sorbitan trioleate	13.3	Yes[b]
	Tween 80	PEG-20 sorbitan monooleate	15.0	No
	Tween 20	PEG-20 sorbitan monolaurate	16.7	No

(a). Nanoemulsions formed for $W_{\%}$>80%. **(b).** Nanoemulsions formed only for $W_{\%}$=80%.

Table 7. Systems essayed in the [0.16 M PBS / CatA : NIS / PLGA 6% in ethyl acetate] at 25ºC. Aqueous content was fixed at 90%. Only method 1 was used in this part.

From all essayed systems, the ones showing higher stability were chosen for further research. Although they were highly stable, research on PBS based systems was discontinued. Research on ethylcellulose-based systems showed that phosphate ions, due to their strong electrolyte character and negative charge, strongly shield the positive surface charge of particles rendering them useless for interaction with anionic biomolecules. Research on systems using Tween 85 as the cosurfactant was also discontinued. These systems were stable only in a narrow region in the ternary phase diagram, and consequently they destabilized when the organic solvent was extracted (the system was moved away from its narrow stability region).

[aqueous phase / CatA : NIS / PLGA 6% in ethyl acetate]

Non-ionic surfactant	Aqueous phase			
	PBS 80 mM	TRIS 50 mM	HEPES 20 mM	Water
Cremophor EL	No [a]	Yes [a,c]	No	Yes [a,c]
Tween 80	No	No	No	No
Tween 85	No [b]	Yes [b]	No	No

(a). Nanoemulsions formed for W%>80%. **(b).** Nanoemulsions formed only for W%>80%. **(c)** Essayed at higher cationic surfactant content with successful results

Table 8. Systems essayed in the [aqueous phase / CatA : NIS / PLGA 6% in ethyl acetate] at 25ºC. Aqueous content was essayed from 80 to 95%.

Nano-emulsions prepared from the [Milli-Q water / CatA:CEL / PLGA 6% in ethyl acetate] and [TRIS / CatA:CEL / PLGA 6% in ethyl acetate] systems proved being the most stable and were further studied by varying cationic surfactant content and characterizing nano-emulsion stability. As shown in Figure 9, for nano-emulsions of the [aqueous phase / CatA:CEL / PLGA 6% in ethyl acetate] system, a higher cationic surfactant content lead to greater droplet sizes. When Milli-Q water was used as the aqueous phase, droplet radii were greater than when using TRIS. This can be attributed to osmotic shrinkage effects due to the presence of solutes in the TRIS solution (as explained in section 6.1.1.).

Regarding the preparation method, method 2 provided smaller droplet radii. Size differences between methods (Figure 9) may be attributed to the fact that method 2 provides a stepwise addition of the destabilizing cationic surfactant into the system during its formation, gradually increasing the HLB of the system as it is needed (as the aqueous content increases). Larger droplets and lower ζ-potential values were obtained by method 1. By using method 1 no nano-emulsions could be formed for cationic surfactant contents as high as with method 2.

Nano-emulsion stability was assessed visually and by light transmission measurements as a function of sample height and time in the [TRIS / CatA:CEL / 6% PLGA in ethyl acetate] system at 25ºC. Depending on cationic surfactant content, it took between 1 day for systems with a surfactant composition of CatA:CEL= 5:1 to more than one month for systems with a surfactant composition of CatA:CEL= 0:1 to visibly start sedimenting. As for any other system studied in this work, a higher cationic surfactant content lead to a faster sedimentation (possibly explained by equation 5). Systems with a surfactant composition of CatA:CEL = 1:1 took about one week to visibly start sedimenting. The nano-emulsions of the [TRIS / CatA : Tween85 / PLGA 6% in ethyl acetate] system at 25ºC showed the highest stability. Figure 10 shows some representative light transmission spectra of the nano-emulsions studied.

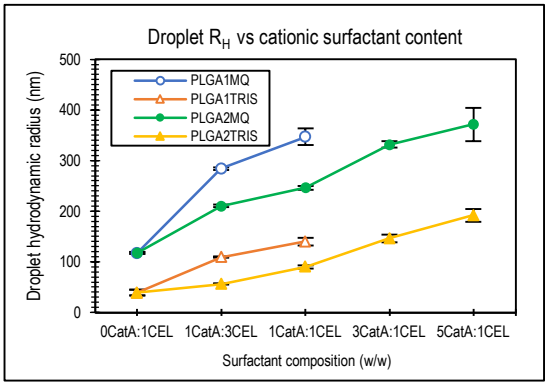

Figure 9. a) droplet size versus cationic surfactant content for the [aqueous phase / CatA:CEL / PLGA 6% in ethyl acetate] at 95% aqueous phase content ant 25ºC. MQ is the abbreviation for Milli-Q ® water. 1 or 2 indicates preparation method 1 or 2.

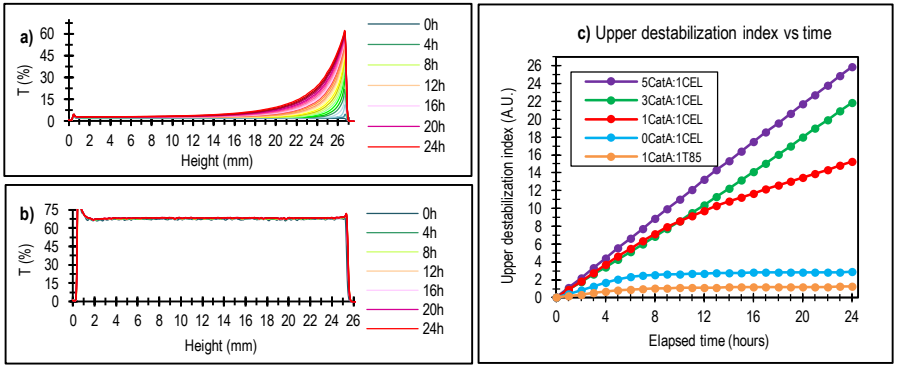

Figure 10. Transmittance vs sample height for the [TRIS / CatA:CEL / PLGA 6% in ethyl acetate] with 95% TRIS at 25ºC and a surfactant composition of CatA:CEL = 5:1 (a) and CatA:CEL = 0:1 (b).

c) Destabilization index vs time for the [TRIS / CatA:CEL / PLGA 6% in ethyl acetate] system with 95% TRIS at 25ºC. The [TRIS / CatA:Tween85 / PLGA 6% in ethyl acetate] system with 95% TRIS at 25ºC is included as 1CatA:1T85 for comparison.

6.2.2. Formation and characterization of nanoparticles

Nanoparticles on the [Milli-Q water / CatA:CEL / PLGA 6% in ethyl acetate] and [TRIS / CatA:CEL / PLGA 6% in ethyl acetate] systems were prepared from template nano-emulsions with an O/S ratio of 70:30 and 95% aqueous phase content at increasing CatA:CEL ratios. The

nano-emulsion templates were prepared by the two methods described in section 5.3.2. at 25ºC.

Particle sizes and Z-potentials are shown in Figure 11. Regarding particle sizes (Figure 11a), there is a clear increase in size as the cationic surfactant content is increased independently on either the method or the aqueous phase used. The explanation for this phenomenon could be HLB-related and is the same as for ethylcellulose-based systems (see section 6.1.2).

Nanoparticle's ζ-potential (Figure 11b) also greatly increased with cationic surfactant content. As for EC-based systems, this could be due to a higher density of surfactant cations on the particles' surface.

Significant differences were found between preparation methods. ζ-potentials of equivalent nanoparticles systems were slightly lower when prepared by method 2 (Figure 11b). The usage of this method also lead to smaller particle sizes which, in turn, allowed for kinetically stable systems to form at higher cationic surfactant contents than through method 1. This allowed preparing nano-emulsions with higher ζ-potentials when using method 2.

Lower ζ-potentials obtained by method 2 could be caused by a higher proportion of cationic surfactant left in the continuous phase at the end of the emulsion formation, but further research must be done to confirm this hypothesis.

When compared to nanoparticle dispersions with ethylcellulose, PLGA-based nanoparticles lead to similar ζ-potentials but slightly greater particle sizes, resulting in a lower stability.

Regarding the aqueous phase of the nanoparticle dispersions, Milli-Q water lead to clearly higher ζ-potentials but also to greater particle sizes. This can be explained by the absence of any solute in ultra-pure water.

Due to their higher stability, nanoparticle dispersions in the [TRIS / CatA:CEL / PLGA 6% in ethyl acetate] systems were chosen for seroalbumin interaction studies at surfactant compositions of CatA:CEL = 1:1 and 1:3.

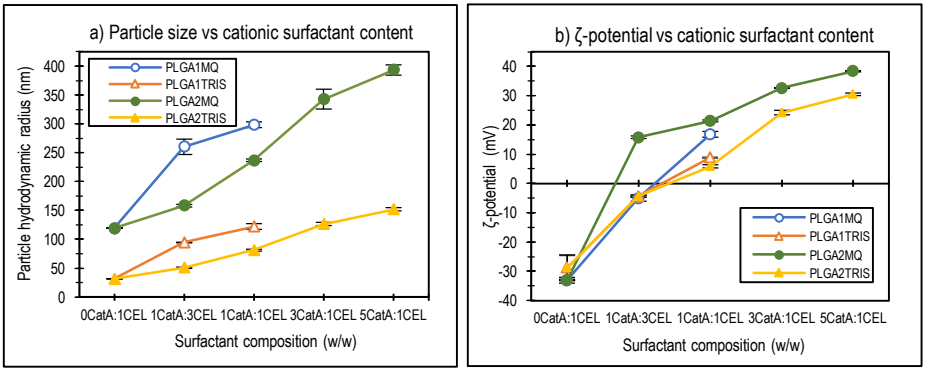

Figure 11. a) Particle size versus cationic surfactant content for the [aqueous phase / CatA:CEL / PLGA 6% in ethyl acetate] system at 95% aqueous phase content and 25ºC. b) Z-potential versus cationic surfactant content for the [aqueous phase / CatA:CEL / PLGA 6% in ethyl acetate]. MQ is the abbreviation for Milli-Q ® water. 1 or 2 indicates preparation method 1 or 2.

6.3. INTERACTION OF NANOPARTICLES WITH BOVINE SEROALBUMIN

The interaction of selected nanoparticle dispersions described above, with bovine serum albumin was studied in vitro in a model simulated blood serum. Serum albumin is the main protein present in blood. The adhesion of proteins to nanoparticles in blood determines its permanence in the blood stream. Serum albumin is considered a disopsonin, thus enhancing blood circulation time when adhering to nanoparticles.

6.3.1. Interaction of ethylcellulose-based nanoparticles with bovine seroalbumin

Interaction of ethylcellulose nanoparticle dispersions of the [TRIS / CatA:CEL / EC 6% in ethyl acetate] system with bovine serum albumin was studied as described in section 5.3.6. The surfactant compositions of the nanoparticle dispersions were CatA:CEL = 1:1 (Figure 12b) and 3:1 (Figure 12a). As shown in Figure 12a, in the CatA:CEL=3:1 system, at low BSA concentration ζ-potential values drop sharply at increasing BSA concentration suggesting adsorption of BSA to the cationic nanoparticle surface. At concentrations below 10 g/L of BSA, ζ-potential values increase slightly and then reach a plateau close to a value of 0 mV. Concerning the size of the nanoparticle-BSA complex, it is shown that at low BSA concentrations, the complex size increases with BSA concentration. A maximum radius of about 2000nm is reached at BSA concentrations of about 6 g/L, and then decreases gradually at

increasing BSA concentration. The maximum in the complex size is reached at BSA concentration values close to the minimum of ζ-potential, as shown in Figure 12a. Two different slopes are observed in the BSA concentration range above 6 g/L.

As shown in Figure 12b, in the CatA:CEL=1:1 system, at low BSA concentration ζ-potential values drop sharply at increasing BSA concentration suggesting adsorption of BSA to the cationic nanoparticle surface. ζ-potential then shows a slight change in slope at 2 to 4 g/L of BSA and then continues to drop until a final plateau is reached.

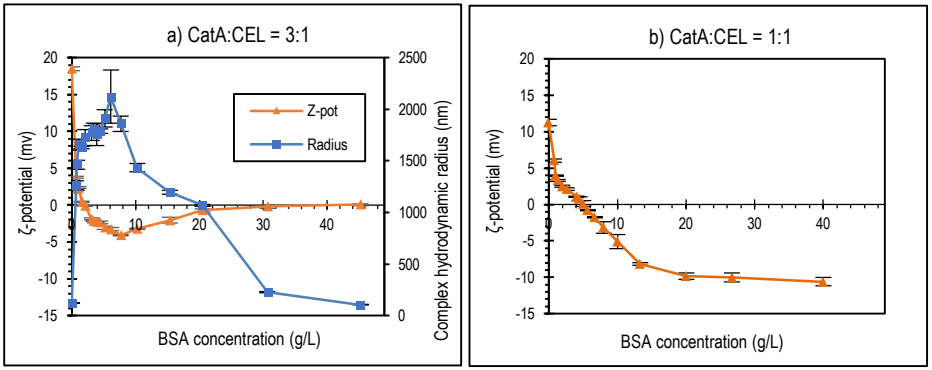

Figure 12. ζ-potential and hydrodynamic radius of nanoparticle-BSA complexes versus BSA concentration, for nanoparticle dispersions of the [TRIS / CatA:CEL / EC 6% in ethyl acetate] system with surfactant composition a) CatA:CEL= 3:1. b) CatA:CEL of 1:1.

This behaviour can be attributed to a strong adsorption of the BSA molecule even at low BSA concentration causing the sharp decrease in ζ-potential and the notable size increase for the CatA:CEL= 3:1 system. At a critical BSA concentration, BSA molecules reorganize in both systems changing their orientation onto the nanoparticle surface, which produces new changes in the size and ζ-potential values of the complexes [14]. Since saturation of the surface occurs at a much lower concentration for the CatA:CEL = 3:1 system, than for the CatA:CEL = 1:1 system this secondary reorganization of BSA molecules probably cannot be observed from the present data for this system.

For both systems, the first decrease in size can be attributed to constriction of the particle by the protein molecules, that then could start changing their orientation to their high concentration orientation (Figure 13) and thus size reaches a slight plateau. With all BSA molecules in their high-density orientation, size starts decreasing again by particle constriction to achieve a final

plateau where no more molecules can be adsorbed, nor more constriction can occur [14]. As stated by Olivier et al [20], high complex hydrodynamic radius values, as those observed in Figure 12a, can be attributed to a multi-layered BSA absorption pattern.

Figure 13. Concentration dependant bovine serum albumin orientations (right). Molecule dimensions of the bovine serum albumin molecule (left). Adapted from reference [14].

6.3.2. Interaction of PLGA-based nanoparticles with bovine seroalbumin

Figure 14 shows the BSA adsorption isotherms by means of particle size and ζ-potential values at increasing BSA concentration for the PLGA nanoparticle dispersions in the [TRIS / CatA:CEL / PLGA 6% in ethyl acetate] system with 95% TRIS and CatA:CEL = 1:1 (Figure 14a) or CatA:CEL = 3:1 (Figure 14b).

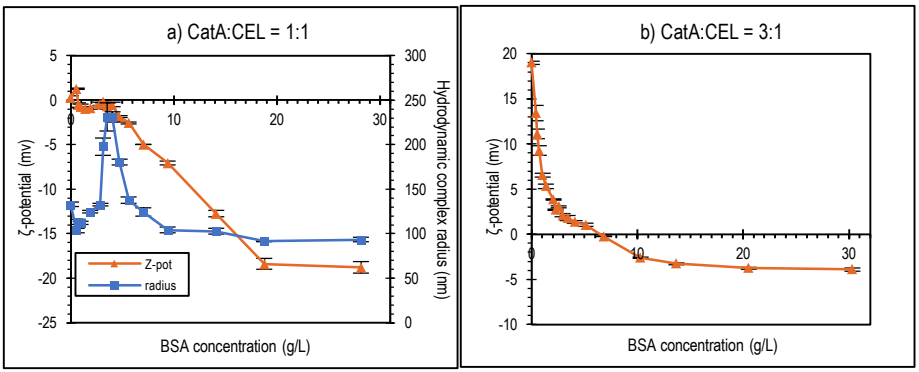

Figure 14. BSA adsorption isotherms as determined by ζ-potential and particle size versus BSA concentration for nanoparticles in the [TRIS / CatA:CEL / PLGA 6% in ethyl acetate] system with 95% TRIS at a) CatA:CEL=1:1. b) CatA:CEL=3:1.

The isotherms suggest that interaction takes place between BSA and the nanoparticle surface. As shown in Figure 14a, at low BSA concentration ζ-potential first increases slightly and then decreases as BSA concentration increases, showing two plateaus, consistent with

BSA reorientation explained above. A similar behaviour (with two plateaus) is observed for the CatA:CEL = 3:1 system (Figure 14b).

The fact that the first plateau in ζ-potential is visible for both PLGA-based systems studied, even for the strongly charged CatA:CEL = 3:1 system (Figure 14b), could indicate a weaker interaction between PLGA and BSA than between ethylcellulose and BSA.

10. CONCLUSIONS

The main objective of this work was to prepare and characterize cationic polymer nanoparticles from template nano-emulsions prepared by the PIC method and assess their interaction "in vitro" with serum albumin. Two different pharmaceutical polymers have been investigated, ethylcellulose and PLGA.

For ethylcellulose-based systems:

- Nano-emulsions have been successfully obtained in the [aqueous component / CatA:CEL / 6% EC in ethyl acetate] system at an O/S ratio of 70/30 and 95% aqueous component, using diluted PBS or TRIS as the aqueous component and varying CatA:CEL ratios, with hydrodynamic radii typically below 150 nm. Droplet size increased with CatA content.
- The nano-emulsions showed suitable stability for nanoparticle preparation. The main destabilization mechanism was sedimentation. Stability of the nano-emulsions decreased at increasing CatA content.
- The nanoparticles prepared from the nano-emulsion templates showed smaller sizes than their template nano-emulsions and positive ζ-potential values when sufficient CatA was present in the surfactant mixture at the studied ratios. When PBS was the aqueous component, particle size and ζ-potential decreased at increasing electrolyte concentration.

For PLGA-based systems:

- Nano-emulsions have been successfully obtained in the [aqueous component / CatA:CEL / 6% PLGA in ethyl acetate] system at an O/S ratio of 70/30 and 95% aqueous component, using water or 50mM TRIS as the aqueous component and varying CatA:CEL ratios, with hydrodynamic radii typically below 400nm.

- When CatA was mixed with TRIS instead of mixing it with the non-ionic surfactant, nano-emulsions showed smaller droplet sizes and could form at higher CatA:CEL ratios.
- The nano-emulsions showed suitable stability for nanoparticle preparation. The main destabilization mechanism was sedimentation. Stability of the nano-emulsions decreased at increasing CatA content.
- The nanoparticles prepared from the nano-emulsion templates showed smaller sizes than their nano-emulsion templates and positive ζ-potential values when sufficient CatA was present in the surfactant mixture at the studied ratios. When the aqueous component was water, ζ-potential of the nanoparticles was higher. When Cat A was dissolved in the aqueous phase ζ-potential of the nano-particles was less positive.

Concerning the interaction of nanoparticles with bovine serum albumin:

- Both, ethylcellulose and PLGA nanoparticles studied showed strong interaction with BSA. Saturation concentration was attained below 8 g BSA/L.

11. REFERENCES AND NOTES

[1]. Anton, N.; Benoit, J.; Saulnier, P., Design and production of nanoparticles formulated from nanoemulsion templates – A review. *J. Controlled Release*, **2008**, 128, 185-199.

[2]. Solans, C.; Solé, I., Nano-emulsions: formation by low-energy methods. *Curr. Opin. Colloid Interface Sci.,* **2012**, 17, 246-254.

[3]. Botet, R., The "Ouzo Effect", recent developments and applications to therapeutic drug carrying. *J. Phys. Conf. Ser.,* **2012**, 352-358.

[4]. Hessien, M.; Singh, N.; Kim C.; Prouzet, E., Stability and tenability of O/W nanoemulsions prepared by phase inversion composition. *Langmuir*, **2011**, 27, 2299-2307.

[5]. Klaus, A. et al., Effect of salts on the phase behaviour and the stability of nano-emulsions with rapeseed oil and an extended surfactant. *Langmuir*, **2012**, 28, 8318-28.

[6]. Fornaguera, C.; Calderó, G.; Solans, C., Electrolytes as a tuning parameter to control nanoemulsions and nanoparticle size. *RSC. Adv*., **2016**, 6, 58203-58211.

[7]. Yukuyama, M.N.; Ghisleni, D.D.M.; Pinto, J.A.; Bou-Chacra, N. A., Nanoemulsion: process selection and application in cosmetics – A review. *J. Cosmetic Sci*., **2016**, 38, 13-24.

[8]. Soppimath, K.S.; Aminabhavi, T.M.; Kulkarni, A. R.; Rudzinsky W.E., Biodegradable polymeric nanoparticles as drug delivery devices. *J. Controlled Release*, **2001**, 38, 1-20.

[9]. Calderó, G.; García-Celma, M. J.; Solans, C., Formation of polymeric nano-emulsions by a low-energy method and their use for nanoparticle preparation. *J. Colloid Inteface Sci*., **2011**, 353, 406-411.

[10]. Masushara, H.; Nakanishi, H.; Sasaki, K. *Single Organic Nanoparticles*. Springer-Verlag, Berlin, **2003**.

[11]. Antonetti, M.; Landfester, K., Polyreactions in miniemulsions. *Prog. Polym. Sci*., **2002**, 27, 689-757.

[12]. Peng, L.; Liu, C.; Kwan, C.; Huang, K. Optimization of water-in-oil nanoemulsions by mixed surfactants. *Colloids and Surfaces A: Physicochem. Eng. Aspects*, **2010**, 370, 136-142.

[13]. Maai, A.; Hamed-Mosavian, M. T., Preparation and application of Nanoemulsions in the last decade (2000-2010). *J. Dispersion Sci. Techol*., **2012**, 34, 92-105.

[14]. Fornaguera, C.; Calderó, G.; Mitjans, M.; Vinardell, M.P.; Solans, C.; Vauthier, C., Interactions of PLGA nanoparticles with blood components: proteïn adsorption, coagulation, activation of the complement system and hemolysis studies. *Nanoscale*, **2015**, 7, 6045 – 6058.

[15]. Pecora, R.; Dynamic Light Scattering: Application of photon correlation spectroscopy. Plenum Press, New York, **1985**

[16]. Swan, J.W.; Furst, E.M., A simpler expession for Henry's function describing the electrophoretic molbility of spherical colloids. *J. Colloid Inteface Sci*., **2012**, 388, 92-94.

[17]. Vauthier. C *et al*, The design of nanoparticles obtained by solvent evaporation: a comprehensive study. *Langmuir*, **2003**, 19, 9504-9510.

[18]. Vittaz, M. et al, Effect of PEO surface density on long-circulating PLA-PEO nanoparticles which are very low complement activators. *Biomaterials*, **1996**, 17, 1575-1581.

[19]. S. Leitner, PhD thesis, Universitat de Barcelona, Barcelona, 2011.

[20]. Olivier, J.C.; Vauthier, C.; Taverna, M.; Ferrier, D.; Courveur, P., Preparation and characterization of biodegradable poly(isobutylcyano acrylate) nanoparticles with surface modified by the adsorption of proteins. *Colloids Surf. B*, **1995**, 4, 349-256.

[21]. [Ethocel™ Standard 10 Premium specification datasheet from Dow Chemicals. https://www.dow.com/en-us/products/ethocel#sort=%40gtitle%20ascending. [Accessed May 17th 2018].

[22]. Rowe, R.C.; Sheskey, P.J.; Quinn, M.E., Handbook of Pharmaceutical Excipients, 6th edition, Pharmaceutical Press, London, **2009.**

[23]. Anderson, J.M.; Shive, M.S., Biodegradation and biocompatibility of PLA and PLGA microspheres. *Adv. Drug Delivery Rev*., **2012**, 64, 72-82.

[24]. Inactive Ingredient Search Page. Food and Drug Administration. https://www.accessdata.fda.gov/scripts/cder/iig/index.cfm?event=BasicSearch.page [Accessed May 23rd 2018].

[25]. The United States Pharmacopeia, 21st revision, The National Formulary, 16th edition, United States Pharmacopeial Convention Inc., Rockville, **1985.**

[26]. Majorek et al, Structural and immunologic characterization of bovine, horse, and rabbit serum albumins. *Mol. Immunol*., ***2012***, 52, 174-182.

[27]. Sah, H., Microencapsulation techniques using ethyl acetate as a dispersed solvent: effects of its extraction rates on the characteristics of PLGA microspheres. *J. Controlled Release*, **1997**, 14, 6085-6092.

12. ACRONYMS

3D-DLS 3D Dynamic Light Scattering

3D-PCS 3D Photon Correlation Spectrometer

BSA Bovine Serum Albumin (or seroalbumin)

CatA Cationic surfactant A (Varisoft RTM 50)

CEL Cremophor EL

R_H Hydrodynamic Radius

DLS Dynamic Light Scattering

EC Ethylcellulose

EC10 ETHOCEL™ STANDARD 10 PREMIUM

HEPES N-(2-hydroxyethyl)piperazine-1-ethanesulfonic acid

HLB Hydrophile Lipophile Balance

NE Nano-emulsion(s)

NIS Non-ionic surfactant

NP Nanoparticle(s)

O/W Oil-in-Water (emulsion)

PBS Phosphate Buffered Saline

PEG Poly(ethylene glycol) also known as macrogol

PIC Phase Inversion Composition Method

PIT Phase Inversion Temperature Method

PLGA Poly(D,L-lactide-co-glicolide) acid

TRIS Tris(hydroxymethyl)aminomethane

W/O Water-in-Oil (emulsion)

APPENDICES

APPENDIX 1: FURTHER DESCRIPTION OF THE MATERIALS USED

A1.1. Surfactants

Ricinoleamidopropyltrimonium methosulfate

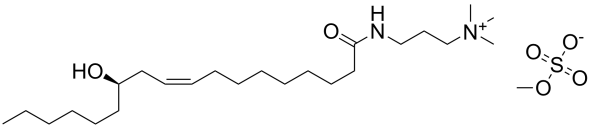

Figure 1'. Structural formula of Ricinoleamidopropyltrimonium methosulfate

Cationic surfactant ricinoleamidopropyltrimonium methosulfate (in the following, abbreviated CatA), commercial name: Varisoft® RTM 50, was obtained from Evonik Rohm GmbH. It is a quaternary amidoamine derivative of ricinoleic acid (the main fatty acid in castor oil) with a high HLB number. It is presented as a viscous and clear yellow liquid with a faint but characteristic castor oil odour. As a cationic surfactant, it is readily soluble in water and is mainly used in softeners, namely, hair and skin softeners. It has been chosen for this work due to the positive surface charge that it can give to nano-emulsions and nanoparticles.

PEG-35 Castor Oil (Kolliphor® EL)

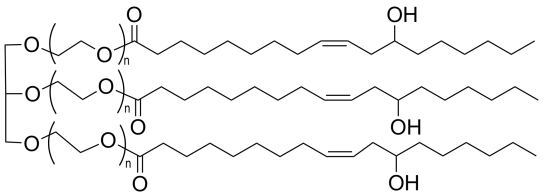

Figure 2'. Structural formula of PEG-35 Castor Oil.

Non-ionic surfactant PEG-35 Castor Oil, commercial name Kolliphor® EL, was purchased from BASF GmbH. It is a polyethoxylated castor oil derivative obtained from the reaction of 35

mole of ethylene oxide with one mole of castor oil. It is presented as viscous liquid with a clear yellow appearance and is readily soluble in water and organic solvents. It has an HLB number of 12 to 14 making it suitable for solubilisation or emulsification of highly hydrophobic components such as drugs or polymer solutions in aqueous buffer solutions. In this work, it will be referred to as CEL since its former commercial name was Cremophor® EL.

Other surfactants

In the following Table, a brief description of other surfactants used during the development of this work can be found.

Chemical Family	Comercial name	Chemical Name	HLB
Polyoxyethylene fatty alcohol ether (non-ionic)	Brij 92V (Fluka)	Polyoxyethylene oleyl ether	4.9[c]
Polyoxyethylene fatty acid esters (non-ionic)	SP Glicerox 767HC (Croda)	PEG-6 caprylic and capric glycerides	13.2[c]
	Cremophor RH455 (BASF)	Mixture of PEG-40 and 5% propylene glycol	14[b]
Polyglyceryl fatty acid esters (non-ionic)	Cithrol PG 3PR-LQRB (Croda)	Polyglyceryl-3 ricinoleate	3.4[c]
Polysorbates (non-ionic)	Tween 21 (Croda)	PEG-4 sorbitan monolaurate	13.3[a]
	Tween 85 (Croda)	PEG-20 sorbitan trioleate	13.3[a]
	Tween 80 (Croda)	PEG-20 sorbitan monooleate	15.0[a]
	Tween 20 (Croda)	PEG-20 sorbitan monolaurate	16.7[a]

(a) From Croda Home Care product datapage. **(b)** From BASF Care Creations datapage. **(c)** From original container label.

Table 1'. Description on other surfactants used in the present work

A1.2. Polymers

Ethylcellulose

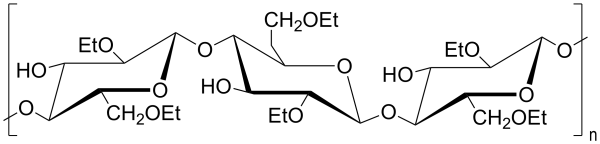

Figure 3'. Ethylcellulose structural formula. Hydrogens are not shown to preserve readability.

Ethylcellulose, trade name: ETHOCEL™ STANDARD 10 PREMIUM (abbreviated as EC), was obtained from Dow Chemicals. It is a polyether presented as a white and loose powder with a density of 1.15 g/cm^3 and a molecular weight of about 65000 g/mol [21]. It is soluble in solvents but insoluble in water. High molecular weight cellulose derivatives are used for oral and topical pharmaceutical formulations. It is considered non-irritating and non-toxic [22], but its parenteral use is controversial due to the fact that it cannot be easily excreted by glomerular filtration.

Poly(D,L-lactide-co-glicolide) acid

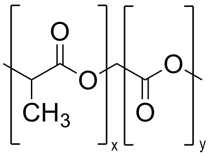

Figure 4'. Schematic representation of PLGA.

Poly(D,L-lactide-co-glicolide) acid, trade name: Resomer RG752H, was obtained from Evonik Rohm GmbH. It is an acid terminated aliphatic polyester presented as a white powder with a density of 1.32 g/cm^3, a molecular weight between 4000 and 15000 g/mol and a polylactic acid content of 75% (molar). It is soluble in polar organic solvents but insoluble in water. It has been chosen for the present work because of its biocompatibility and biodegradability (PLGA is approved by the FDA for parenteral use [22, 23]).

A1.3. Organic solvents and aqueous components

Tris(hydroxymethyl)aminomethane

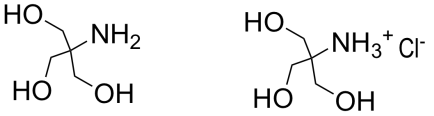

Figure 5'. Structural formula of TRIS buffer components.

Tris(hidroxymethyl)aminomethane, also known as tromethamine and commonly abbreviated TRIS or THAM, was obtained from Sigma (commercial name: Trizma®). It is presented as two separate components, the amino form and its hydrochloride form, both having a white and crystalline powder appearance. By solving different amounts of each component, different pH buffers can be prepared. For this work, a 0.05M buffer with pH = 7.4 at 37 ºC was used. According to the FDA's this pH buffer is suitable for parenteral usage[24] (there are several products containing TRIS currently being sold).

N-(2-hydroxyethyl)piperazine-1-ethanesulfonic acid

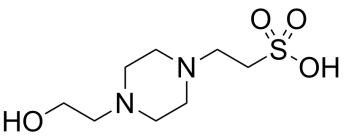

Figure 6'. Structural formula of the HEPES molecule

N-(2-hydroxyethyl)piperazine-1-ethanesulfonic acid, biotechnology performance certified, was purchased from Sigma. It is presented as a hygroscopic white powder and its name is commonly abbreviated as HEPES. A 20 mM buffer with a pH of 7.4 was used in this work. Since it is hypotonic to cells, osmolarity must be adjusted before testing on living cells.

Phosphate buffered saline

Phosphate buffered saline, usually abbreviated as PBS, is a common pH buffer solution in biological research that is suitable for intravenous use [25]. It was prepared by dissolving appropriate quantities of sodium dihydrogen phosphate and disodium hydrogenphosphate and

adjusting the osmolarity with sodium chloride. A final pH adjustment is made with 85% orthophosphoric acid for a final concentration of salts isotonic to cells (160 mM). Lower concentrations were attained by diluting the 160 mM stock solution.

Component [formula]	**Concentration** [g/L]	**Concentration** [mM]
NaCl	8.00	136.9
NaH_2PO_4	0.25	2.1
Na_2HPO_4	2.38	16.7

Table 2'. 160 mM phosphate buffered saline stock solution composition

Ethyl Acetate

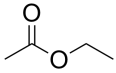

Figure 7'. Structural formula of ethyl acetate

Ethyl acetate (SupraSolv®, for GC-FID) was obtained from Merck. It is a flammable volatile ester (b.p.: 77ºC) with a density of 0.902 g/cm^3 and a fruity and characteristic aroma. It has a refractive index of 1.372 [27] (relevant when performing DLS measurements). It is partially soluble with water:

Mixture	**Solubility** [% w/w]
Ethyl acetate in water	7.39[27]
Water in ethyl acetate	3.30[27]

Table 3'. Solubility data at 25ºC of the ethyl acetate – water system.

Ethyl acetate toxicity is low compared to other organic solvents and can be used in pharmaceutical preparations without any justification in concentrations of up to 5000 ppm [ICH Guidelines, 2011]. In fact, it is also used as food flavouring with the E-number E1504.

A1.4. Biomolecules

Bovine Serum Albumin

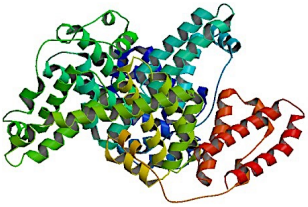

Figure 8'. Bovine serum albumin's 3D structure. From reference [26]

Bovine serum albumin, heat shock fraction ≥98%, was purchased from Sigma. It is presented as lyophilized straw-coloured flakes that dissolve readily in water. Bovine serum albumin, usually abbreviated as BSA, is the major protein in the blood of bovine livestock. Its isoelectric point is 4.7 [26]. Due to their similarities [26], BSA is used as a substitute of human serum albumin in most early stage in vitro essays.